Scripta Materialia 145 (2018) 62–66

Contents lists available at ScienceDirect

Scripta Materialia

journal homepage: www.elsevier.com/locate/scriptamat

Regular article

In-situ TEM study of dislocation emission associated with austenite growth

Juan Du [a], Frédéric Mompiou [b], Wen-Zheng Zhang [a,*]

[a] Key Laboratory of Advanced Materials (MOE), School of Materials Science and Engineering, Tsinghua University, Beijing 100084, PR China
[b] CEMES-CNRS, Université de Toulouse, 29 rue J. Marvig, 31055 Toulouse, France

ARTICLE INFO

Article history:
Received 8 September 2017
Accepted 9 October 2017
Available online xxxx

Keywords:
In-situ TEM
Dislocation emission
Pitsch OR
Austenite/ferrite interface

ABSTRACT

The emission of dislocations from the tip of a newly transformed austenite lath, with a near Pitsch orientation relationship with the ferrite matrix, was observed at 760 °C in a duplex stainless steel, using in-situ transmission electron microscopy. The dynamics of dislocation loops with $[111]_b/2$ Burgers vector were carefully analyzed. An estimation of stress concentration at the tip was made using dislocations as stress probes. These real-time observations verify directly for the first time that dislocation activity assists the growth of austenite precipitates, and provide quantitative data for revealing the stress field generated by interface migration.

The phase transformation between austenite (fcc) and ferrite (bcc) is one of the most important solid-state transformations because of its practical importance as a metallurgical tool to tailor the mechanical properties of steels. A fundamental step to understand the phase transformation is to study interfacial structures between product and matrix phases. Although numerous experimental and theoretical studies have been made on the structure of fcc/bcc interfaces [1–13], only few in-situ experiments have been conducted to directly observe the interface migration [14,15]. There are considerable and persuasive evidence that the phase transformation is frequently associated with dislocation activity, especially when the product phase exhibits a plate, lath or needle shape. It has been reported that matrix dislocations connect with growth ledges in a Ni-Cr-alloy [1,16,17] and that matrix dislocations interconnect precipitate needles throughout the matrix in a Fe-Cu alloy [2]. An in-situ transmission electron microscopy (TEM) study has revealed the emission of dislocations both in austenite and ferrite to release stress near the transformation front during the decomposition of Fe-C austenite [15]. However, the details of dislocation activity associated with the moving interface remain unclear, and a complete dislocation characterization is still lacking in the previous work. The dislocation activity is probably due to a long-range stress field caused by the phase transformation. Therefore, a detailed description of the dislocation activity may shed some light on this stress field, which is often uneasy to measure quantitatively.

* Corresponding author.
E-mail address: zhangwz@mail.tsinghua.edu.cn (W.-Z. Zhang).

In this study, we carried out in-situ TEM experiments to observe directly growth of fresh austenite from ferrite matrix in a duplex stainless steel, and tracked dislocation activity associated with the interface migration. Fe-24.9Cr-7.0Ni-3.1Mo (wt%) alloy was used in the present work. 10 mm × 10 mm × 10 mm alloy blocks were encapsulated in silica tubes for a solution treatment at 1300 °C for 30 min, followed by water quenching so that ferrite phase could be preserved at room temperature. TEM sample preparation was obtained by mechanical thinning and twin-jet polishing (with an electrolyte of 8 vol% perchloric acid in ethanol at −30 °C and with an applied voltage of 20 V). In-situ TEM experiments were performed in a Philips CM20FEG microscope operated at 200 kV using a GATAN heating holder. Samples were heated first at the highest temperature rate (several °C/s) up to 700 °C, and then slowly heated by 5 °C increments until the first fresh austenite was noticed. The interface motions were recorded using a Gatan Orius side entry camera operated at 15 fps. After in-situ experiments, crystallographic features were determined by a Kikuchi line analysis, with an average misorientation error of ±0.5°. All crystallographic indexes are self-consistent with a selected variant of the orientation relationship (OR).

Upon heating, fresh austenite precipitates are formed by nucleation and growth from the ferrite matrix. As in bulk materials, the fresh austenite in thin TEM foils also exhibits a lath morphology, with the long axis lying approximately in the foil. The observations reported below focus on the phenomena of growth close to the moving tip.

Fig. 1 shows a series of bright field images extracted from a video sequence (see Supplementary movie S1) taken at 760 °C, with the time for Fig. 1a being arbitrarily set at $t = 0$ s. It can be seen from Fig. 1 that besides the foil surfaces the growing austenite lath is enclosed by two near

https://doi.org/10.1016/j.scriptamat.2017.10.014
1359-6462/

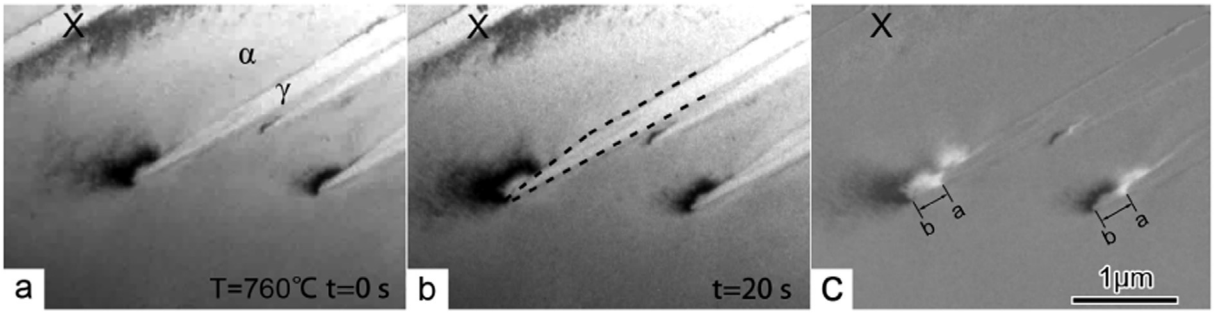

Fig. 1. Wedge-shaped tip of austenite (γ) lath growing in ferrite (α) matrix at 760 °C: a) $t = 0$ s; b) $t = 20$ s. c) is the image difference a)–b) highlighting the growth of the austenite lath. X is a reference marker. See Supplementary movie S1 for details.

parallel flat interfaces and one inclined interface, resulting in a wedge tip. Using X as a fiducial marker, the overall tip migration along the long axis can be measured from the image difference between Fig. 1a and b, as given in Fig. 1c. An average growing rate of 15.6 nm/s is estimated. A bending contour adjacent to the inclined interface at each tip was observed during the motion. The location of the bending contour suggests an asymmetrical stress field near the migrating tip. For this case, no dislocation activity was observed. A probable reason is that the stress field at the lath tip is below the critical value for dislocation nucleation.

In contrast to the case in Fig. 1, dislocation emission has been observed near the tips of a number of austenite laths. Fig. 2 shows an example of dislocation emission from such a tip. Seventeen dislocation loops were emitted one after another in a similar manner. Fig. 2a–d consist of sequential snapshots (see Supplementary movie S2) of a typical process of the expansion of a dislocation loop at the lath tip. These bright field images were recorded under two-beam condition using $\boldsymbol{g}_{(011)\mathrm{b}}$. The loop is unclosed, with two ends connecting to two sides of the tip. Once generated, the portion of the loop in the immediate vicinity of the tip does not expand to the matrix immediately, but it apparently hesitates to detach from the tip (as seen from the new small loop in Fig. 2c). After leaving from the tip, the dislocation loop expands rapidly ahead of the tip. It indicates that the emitted dislocation is strongly repelled by the stress field present at the lath tip. When the loop meets the foil surface, it breaks into two dislocation segments that leave a visible trace, due to the presence of a thin oxide layer on the surface. The dislocation meets first the upper surface and then the lower surface, yielding traces t_{1u} (Fig. 2b) and t_{1l} (Fig. 2c), respectively. The two dislocation segments, marked by s_1 and s_2 in Fig. 2c, continue to move. While segment s_1 moves away from the tip at a similar rate as the tip-front portion of initial loop, segment s_2 slows down as it moves towards a lath side. After gliding for a certain distance, segment s_1 will cross slip, as evidenced by the change of trace direction (Fig. 2d). The new straight traces on upper and lower surfaces are referred to t_{2u} and t_{2l}, respectively. This indicates that s_1 is largely a screw dislocation. Meanwhile, a new dislocation loop was nucleated, as seen in Fig. 2c. In addition to these continuously generated dislocation loops, several other dislocations were occasionally observed in the vicinity of the tip, without being clearly determined. They present a very weak contrast, indicating that they are out of contrast with this diffraction condition.

Post-mortem crystallographic analysis was made on the austenite lath in Fig. 2. The OR between austenite and ferrite was found near the Pitsch OR [18], i.e., $(100)_f \sim \parallel (110)_b, 0.6^\circ$ and $[0\bar{1}1]_f \sim \parallel [1\bar{1}1]_b, 0.6^\circ$, which was seldom observed in steels (the subscript f and b refer to fcc and bcc lattices, respectively). Fig. 2e illustrates schematically the geometry of the austenite lath and the crystallography of several typical planes of ferrite in Fig. 2a–d. The long axis of austenite lath is $[\bar{1}\ \overline{7.3}\ 6.6]_f \parallel [5.1\ \overline{6.6}\ 5.4]_b$, i.e. lying in the flat interface, with an orientation of $(0.48\ 0.50\ 0.72)_f \parallel (0.08\ 0.61\ 0.79)_b$. The measured foil normal is $(0.85\ 0.38\ \overline{0.36})_b$. Based on the measured directions of slip traces and widths between traces on the upper and lower surfaces, the slip planes were determined as $(11\bar{2})_b$ and $(10\bar{1})_b$, respectively (see Supplementary materials for the detailed calculation). The Burgers vector of the emitted dislocations is thus determined as the intersection of these two planes, namely $\boldsymbol{b} = [111]_b/2$. This result is consistent with the diffraction contrast of the dislocation under $\boldsymbol{g}_{(011)\mathrm{b}}$ in Fig. 2.

In order to analyze the tip motion, a custom made script was used to track the tip position in Fig. 2. To avoid artifacts due to the contrast changes when the dislocations are emitted, the tip motion was analyzed manually by image difference during a short period of time around the dislocation emission. The displacement of the tip along the long axis versus time is given in Fig. 3. The time reference is chosen as the moment of the dislocation being emitted in Fig. 2a. It can be seen from Fig. 3 that the moving rate is almost constant (7–8 nm/s), but with several decelerations shown as kinks on the displacement curve. The change in tip velocity is concomitant with dislocation emission noted by D in Fig. 3. The jerky nature of the tip moving rate is probably due to the accumulation and relaxation of stress field near the tip. The emission of a dislocation loop from the tip may also affect tip moving rate via interaction between the local dislocation loop and the possible interfacial dislocations in the semicoherent interface surrounding the tip. Consequently, the tip halted temporarily. It has been checked that the length and width of austenite lath in Fig. 1 are both smaller than those in Fig. 2, and the foil containing the lath in Fig. 1 is also thinner. In this sense, though the austenite lath in Fig. 1 shares a similar OR with that in Fig. 2, the stress accumulated near the tip could be smaller. This might be a reason why the growth of the small laths in Fig. 1 is not associated with dislocation activity.

Dynamics of dislocations can be explained according to an analysis of dislocation displacement. Fig. 4 shows image differences at difference time intervals between snapshots extracted from the video (see Supplementary movie S2). Dislocations numbered D1 to D5 in Fig. 4a–d show white and black contrasts before and after. Accordingly, the displacement between white and black contrasts can be used to estimate the average moving rate of dislocations. The net shear stress acting on each dislocation results from a combination of the stress field at the lath tip (τ_{tip}), the image stress tending to attract the dislocation loop to the surface (τ_{image}), the line tension (τ_l) and the interaction stress between dislocations (τ_{inter}). As can be seen from Fig. 4a, dislocation D1 moves first rapidly mainly due to the τ_{tip} and crosses a zone about 200 nm ahead of the tip. The shear stress required to nucleate the loop can be evaluated by measuring the loop size at the critical configuration before loop expansion, i.e. when τ_{tip} is comparable to τ_l (i.e. neglecting τ_{image} and τ_{inter}).